X-ray diffraction studies of the crystallization of phase change nanoparticles produced by self-assembly-based techniques

Simone Raoux[1], Yuan Zhang[2], Delia Milliron[1], Jennifer Cha[1], Marissa Caldwell[2], Charles T. Rettner[1], Jean L. Jordan-Sweet[3], and H.-S. Philip Wong[2]

[1] IBM Almaden Research Center, 650 Harry Road, San Jose, CA 95120
[2] Department of Electrical Engineering and Center for Integrated Systems, Stanford University, 420 Via Palou, Stanford, CA 94305
[3] IBM T. J. Watson Research Center, P. O. Box 218, Yorktown Heights, NY 10598
e-mail: simone_raoux@almaden.ibm.com

ABSTRACT

The crystallization behavior of phase change nanoparticles can provide useful insight into the scaling properties of phase change materials and of related memory devices. While such nanoparticles can be fabricated using electron-beam lithography, this method is expensive and time-consuming. We have therefore developed fabrication techniques based on self-assembly-based lithographic processes. We have successfully made three types of phase change nanoparticle samples, and have applied time-resolved X-ray diffraction to study their crystallization behavior.
Two kinds of self-assembling diblock-copolymers were applied to pattern the phase change materials. In one case self-assembled PS-b-P4VP (polystyrene-b-polyvinylpyridine) was formed on top of an amorphous GeSb phase change film and was used to locally grow SiO_2 dots on top of the P4VP domains. The SiO_2 dots then served as a hard mask to transfer the pattern into the GeSb film using reactive ion etching and ion milling, and isolated 15 nm diameter dots were formed. It was found that these GeSb nanoparticles have a crystallization temperature that is 15ºC lower than comparable blanket film. In the second case cylindrical-phase PS-b-PMMA (polystyrene-b-poly(methylmethacrylate)) films were used. After removal of the PMMA domains, AgInSbTe phase change material was deposited by sputtering using a substrate rf bias and a collimator for better conformality. After lift-off of the PS, isolated AgInSbTe nanoparticles of about 20nm diameter were obtained that showed a crystallization temperature of 175ºC, slightly higher than blanket film (165ºC).
The same PS-b-PMMA template was used to deposit newly-developed spin-on phase change material. A GeSeSb precursor was synthesized by dissolving GeSe and Sb_2Se_3 in hydrazine in the presence of additional elemental selenium. The template was filled with precursor by spin casting, then annealed to form an array of ~20 nm diameter GeSbSe nanoparticles. Finally, the PS template was dissolved to leave the nanoparticles. These arrays crystallized at about 215°C which is 35 °C lower than a blanket film.
All of these experiments confirm that phase change devices should scale to well below 20nm.

Key words: phase change nanoparticles, scaling

1. INTRODUCTION

Phase change random access memory (PCRAM) is a promising technology that applies phase change materials, which are successfully used in optical storage in re-writable CDs and DVDs, to solid state memory technology. While in optical storage the large change in reflectivity between the amorphous and crystalline phase of these materials is used to store the information, in PCRAM the large (several orders of magnitude) change in resistivity is applied. The state of the PCRAM cell can be switched using current pulses. If the cell is in the high-resistive OFF state a current pulse is applied that heats the phase change material above its crystallization temperature for a long enough duration to transform it into the crystalline state (SET operation). If the cell is in

the low-resistive ON state a typically shorter and higher current pulse is applied that heats the phase change material above its melting point. The current is then switched off quickly and the material is quenched back into the amorphous phase. The reading operation is performed by a low current pulse that does not heat the material to cause any phase change but can detect the resistivity state of the cell.

PCRAM has been demonstrated in a variety of embodiments and using a variety of materials. Most memory cells are of the so-called mushroom type, where a relatively large block of phase change material is contacted by a narrow electrode and only a fraction of the phase change material is switched that is directly above the electrode. Another type of cell is a so-called bridge or line structure, where a narrow stripe of phase change material is contacted on both sides and the center part of the bridge or line is switched. Using electron-beam lithography or techniques that can produce sub-lithographic dimensions of certain features very small prototype cells have been fabricated[1-5].

Scaling behavior of phase change nanoparticles and ultra-thin films has been studied before[6,7]. It was found that phase change nanoparticles with sizes larger than 20nm fabricated by electron-beam lithography show very clear crystallization behavior with crystallization temperatures T_x not very different from thick blanket films. Ultra-thin films were shown to have an increased T_x for films thinner than 10nm and the thinnest films that still show crystallization are in the 2nm thickness range. In the present study we have fabricated phase change nanoparticles of the materials GeSb and AgInSbTe using self-assembling diblock-copolymers and sputter deposition[8,9]. In addition we demonstrate an alternative method for phase change material deposition – spin-coating using newly developed spin-on phase change materials[10]. Using self-assembling diblock-copolymers again as the base for patterning we fabricated phase change nanoparticles by spin-on and lift-off. These fabrication methods offer the possibility to obtain nanoparticles that are smaller than can be achieved by electron-beam lithography and over much larger area for a fraction of the cost. The crystallization behavior of all nanoparticle arrays was investigated using *in-situ*, time-resolved X-ray diffraction (XRD) during sample heating.

2. NANOPARTICLE FABRICATION

First method:
Thin films of the phase change material GeSb (15 at. % Ge, 85 at. % Sb) were deposited by magnetron sputter deposition on Si substrates from a compound target in an Ar flow of 40sccm and a pressure of 0.27Pa using 12W dc power. The films were amorphous with a thickness of 10nm. The composition, which is the eutectic alloy with the lowest melting point, was verified by Rutherford backscattering spectrometry (RBS). The films were capped by a 10nm thick diamond-like carbon (dlc) layer formed by ion beam deposition using a VEECO IBD system run with a 210 mm low power grid which extracts ions from a methane plasma. To enhance adhesion, 0.3 nm of Si was deposited prior to the dlc layer. The dlc layer served as a hard mask for the pattern transfer into the phase change material. A 30nm thick self-assembled PS-b-P4VP (polystyrene-b-polyvinylpyridine) layer was formed on top of the dlc/Si/GeSb film stack by spinning PS-b-P4VP polymer diluted in toluene to weight percentage 0.7wt%. Subsequent solvent annealing in an oven at 65°C (well below the T_x of GeSb at 250ºC) in toluene vapor for more than 10h was performed to promote phase separation and long-range ordering. By exposing the polymer sample to tetraethylorthosilicate (TEOS) and water vapor at a temperature of 65°C for 18-24h, SiO_2 nucleated at the pyridine domains only and grew from the surface forming an ordered array of SiO_2 dots on the surface. Figure 1a shows an SEM image of such an array of highly ordered SiO_2 dots after growing for 24 hours. This pattern was transferred first into the dlc using CO_2 reactive ion etch in a Unaxis etch tool that consumed most of the SiO_2 but patterned the dlc which was then used as a hard mask to transfer the pattern further into GeSb using ion milling. Ion milling was performed in a custom VEECO IBE system using argon ions with an energy of ~200eV and with an angle of 10° while rotating the sample. Etch times of 120s produced well isolated GeSb nanoparticles which are shown in Fig. 1b. The nanoparticles were capped in-situ with a 10nm thick Al_2O_3 layer to prevent oxidation using ion beam deposition at an angle of 45° while rotating the sample. The pattern transfer is described in more detail in refs. 8 and 9. Cross-sectional TEM was used to

confirm that the nanoparticles were indeed well isolated. The size of the nanoparticles was about 15nm, which is smaller than the GeSb nanoparticles fabricated previously by electron beam lithography[7].

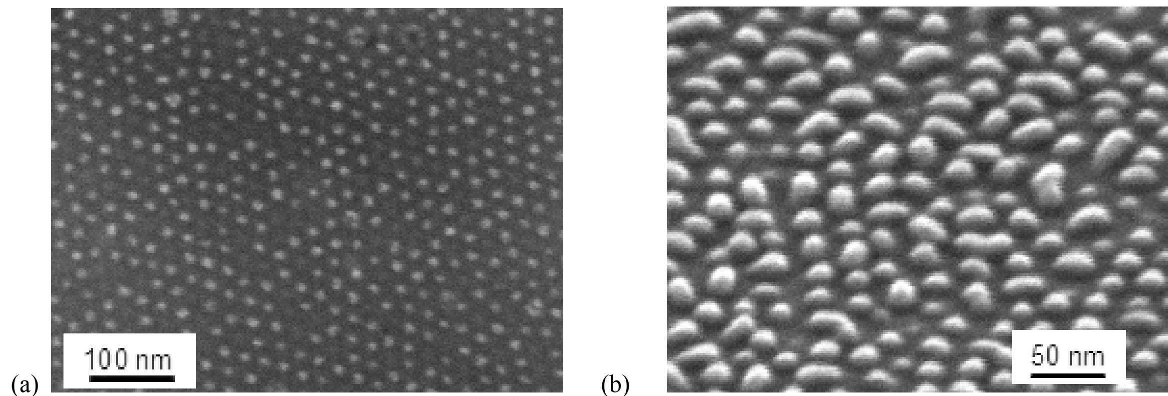

Figure 1: (a) SEM image of well-ordered SiO_2 dots grown on top of the pyridine domains of a self-assembled PS-b-P4VP layer on top of a dlc/Si/GeSb film stack. (b) SEM image of isolated GeSb nanoparticles fabricated by the first method.

Second method:

In the second approach to fabricate phase change nanoparticles cylindrical-phase PS-b-PMMA (polystyrene-b-poly(methylmethacrylate)) films were used to form a self –assembly pattern on Si substrates. Random copolymer was first spun on the Si substrate to neutralize the surface, followed by spin-on of the PS-b-PMMA. After the self-assembly of the block copolymer film, the PMMA was displaced with acetic acid, leaving an array of nanoscale holes. Then, the bottom of the holes were cleared down to the substrate using a 5s oxygen plasma etch to remove the underlying random copolymer layer. Ag and In doped Sb_2Te (AIST) was deposited from a compound target using magnetron sputter deposition in 40sccm Ar flow at a pressure of 0.27 Pa and a dc power of 12W. A collimator with an aspect ratio of 1:1 was placed between the sputter gun and the sample to improve directionality of the deposition. The film thickness was 20nm and the film composition was Ag:In:Sb:Te = 7 at.% : 11 at.% : 48 at.% : 34 at.% with an accuracy of ± 5 at.% determined by RBS (Ag:In:(Sb+Te) ratios) and Particle Induced X-ray Emission PIXE (Sb:Te ratio). The AIST film was capped by an 8nm thick SiO_2 layer also deposited by magnetron sputtering using 200W rf power. Finally, the AIST nanoparticles were exposed by lift-off of the PS template with toluene. Figure 2a shows the PS/PMMA template after AIST/SiO_2 deposition before lift-off, and Fig. 2b shows the 20nm AIST nanoparticles after lift-off.

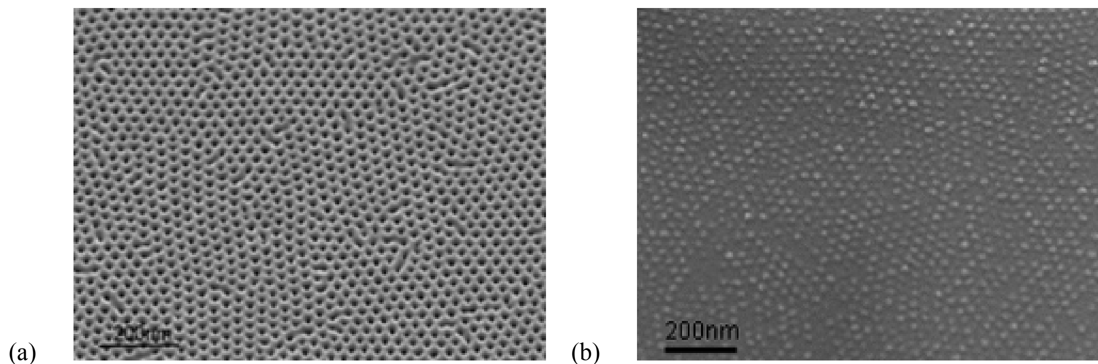

Figure 2: (a) PS/PMMA template after AIST/SiO_2 deposition before lift-off. (b) AIST nanoparticle array after lift-off.

Third method:
The same PS-b-PMMA template was used to deposit newly-developed spin-on phase change material[10]. A GeSeSb precursor was synthesized by dissolving GeSe and Sb_2Se_3 in hydrazine in the presence of additional elemental selenium. Removing the hydrazine under flowing nitrogen, a solid precursor was recovered which was redissolved in dimethylsulfoxide/ethanolamine to process into thin films. RBS analysis of precursor powders and thin films annealed at or above 160 °C detected no residual nitrogen within a detection limit of 5%. Again the PS/PMMA template was etched leaving the template hydrophilic, which facilitates deposition of the phase change precursor. The template is filled with precursor by spin casting a dimethylsulfoxide/ethanolamine solution, then annealed at 160ºC to form an array of ~20 nm diameter amorphous GeSbSe nanodots on the silicon surface. The final nanopatterned array is formed again by lift-off. Figure 3a shows an SEM image of the GeSbSe nanoparticles after lift-off, and Figure 3b shows a cross-sectional TEM image of nanoparticles with a composition of $Ge_{5.6}\,Sb_{31.0}Se_{63.4}$ as determined by RBS and PIXE.

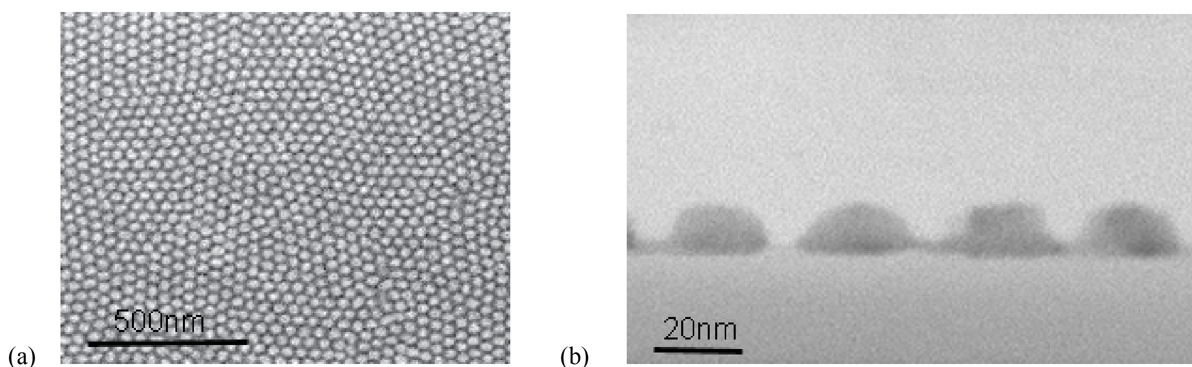

Figure 3: (a) SEM image of the GeSbSe nanoparticles made from spin-on material after lift-off. (b) Cross-sectional TEM image of GeSbSe nanoparticles made from spin-on material.

3. TIME-RESOLVED XRD STUDIES

The crystallization behavior of phase-change nanoparticle arrays was studied using *in-situ* time-resolved X-ray diffraction (XRD) during sample heating. Beamline X20C of the National Synchrotron Light Source at Brookhaven National Laboratory where the experiments were performed is equipped with a high-throughput synthetic multilayer monochromator and fast linear-diode-array detector. A special chamber for controlling the sample ambient (purified He gas) and containing a BN heater for rapid annealing was used to heat the samples at a rate of 1 ^{o}C /s. Simultaneously, the diffracted XRD peak intensities were detected over a 2θ range of 15° selected according to the position of the strongest diffraction peaks of the corresponding crystalline phase change materials using a photon energy of 6.9 keV.
Figure 4b shows the time-resolved XRD peak intensity during a heating ramp of GeSb nanoparticles fabricated by the first method (as shown in Fig. 1) compared to the XRD peak intensity of a GeSb film of 30nm thickness (Fig. 4a). It can be seen that the nanoparticle array shows the appearance of XRD peaks at a temperature of about 235ºC, about 15ºC lower than the appearance of the peaks for blanket film of around 250ºC. As it was observed previously[7], the GeSb XRD peaks can be indexed as a rhombohedral Sb crystal structure. There is a change in texture: the blanket film shows strong texture with the (003) peak being the most intense while the peak intensity of the nanoparticle array resembles more that of a powder pattern with the (012) peak having the highest intensity. This can be explained assuming that the blanket film shows a preferred orientation of one crystalline axis with respect to the substrate surface while for nanoparticles the grain growth likely starts at all interfaces and thus the grain orientation with respect to the substrate surface is more random. We find that the nanoparticles show clear crystallization at a temperature slightly lower than blanket film which is in good agreement with observations on larger GeSb nanoparticles fabricated by electron-beam lithography[7].

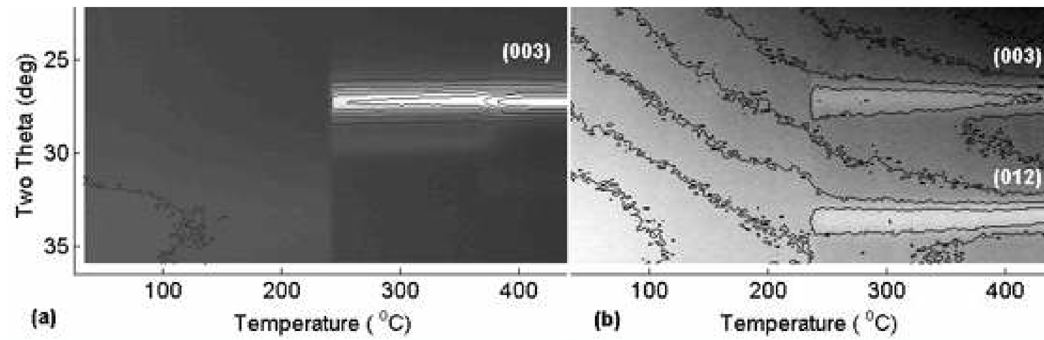

Figure 4: Intensity of diffracted XRD peaks as a function of temperature during a 1ºC/s heating ramp for GeSb film of 30nm (a) and GeSb nanoparticles (b) with 15nm diameter fabricated by the first method and shown in Fig. 1.

Figure 5 shows θ–2θ scans of an AIST nanoparticle array fabricated by the second method (and shown in Fig. 2) compared to 50nm thick blanket film. The nanoparticle array was heated to different temperatures at a rate of 1ºC/s, cooled down, and θ–2θ scans where taken after each heating cycle.

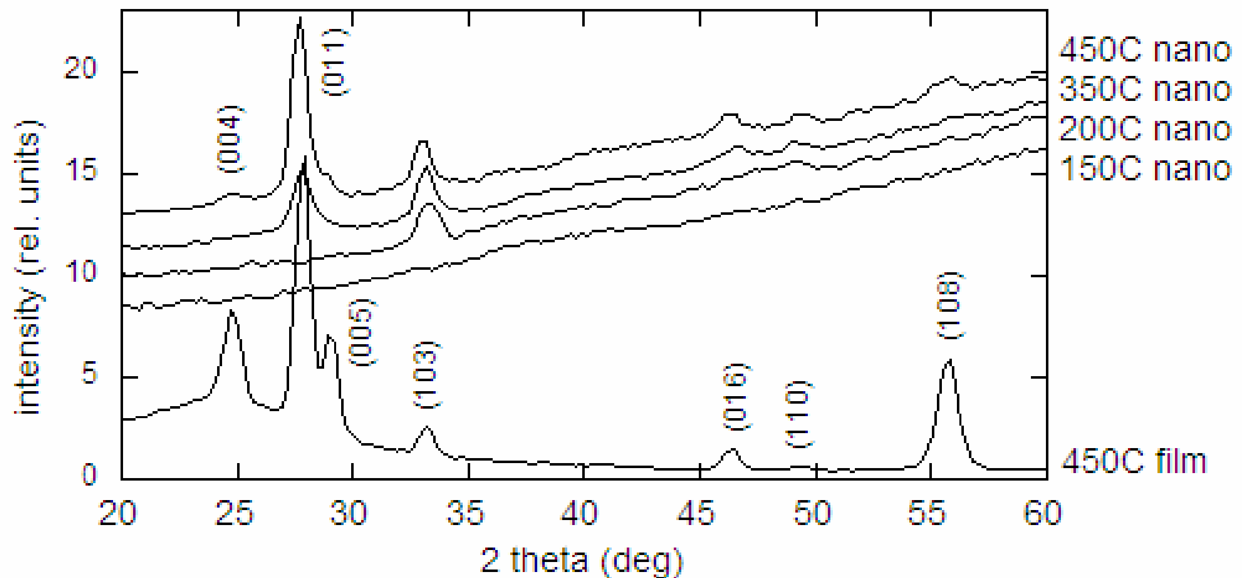

Figure 5: θ–2θ scans of an AIST nanoparticle array ("nano") fabricated by the second method and shown in Fig. 2 compared to 50nm thick blanket film ("film") after heating to various temperatures indicated on the right.

We can see that the nanoparticle array is still amorphous after heating to 150ºC but shows first crystallization peaks after heating to 200ºC. Time-resolved XRD measurements (not shown here) indicate a crystallization temperature of 175ºC. Additional peaks appear after heating to 350ºC and 450ºC, but they can all be indexed as hexagonal Sb_2Te similar to the blanket film. This transition temperature is slightly higher than blanket AIST film which crystallizes at around 165ºC. Again we observe clear crystallization of the nanoparticle array at a temperature which is not very different from the blanket film.

Figure 6 shows the intensity of the diffracted XRD peaks as a function of temperature during a heating ramp with a rate of 1ºC/s of a GeSeSb nanoparticle array fabricated by the third method and shown in Fig. 3 compared to a blanket film.

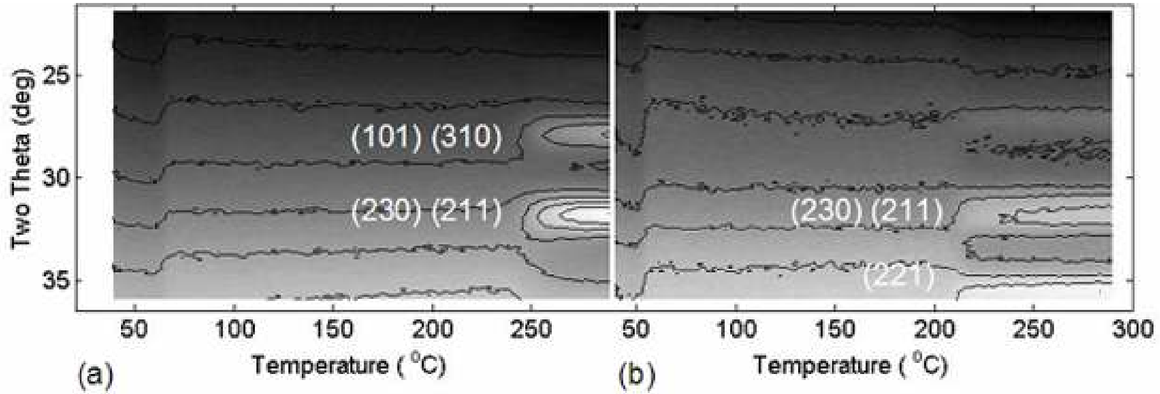

Figure 6: Intensity of the diffracted XRD peaks as a function of temperature during a heating ramp with a rate of 1ºC/s of a GeSb blanket film (a) compared to a GeSeSb nanoparticle array (b) fabricated by the third method and shown in Fig. 3.

Crystallization of the nanoparticle array with a crystallization temperature that is slightly lower (215ºC) than blanket film (250ºC) is clearly observed, combined with some texture change. The θ–2θ scans (not shown here) can be indexed to the orthorhombic structure of Sb_2Se_3. This shows that spin-on phase change materials can have crystallization temperatures in the desired range for solid-state memory applications well above typical memory operation temperatures (80ºC for embedded memory, 150ºC for automotive applications). They also can be scaled to very small dimensions and spin-on phase change nanoparticle arrays crystallize at temperatures not very different from blanket films.

Table 1 summarizes the results on the nanoparticle arrays.

material	fabrication method	deposition method	size (nm)	T_x nano (C)	T_x film (C)
$Ge_{15}Sb_{85}$	subtractive	sputter	15	235	250
$Ag_7In_{11}Sb_{48}Te_{34}$	additive	sputter	20	175	165
$Ge_{5.6}Sb_{31.0}Se_{63.4}$	additive	spin-on	20	215	250

Table 1: Results on the nanoparticle arrays. T_x nano and T_x film are the crystallization temperatures of the nanoparticle arrays and blanket films, respectively.

4. CONCLUSIONS

Phase change nanoparticle arrays of different materials ($Ge_{15}Sb_{85}$, $Ag_7In_{11}Sb_{48}Te_{34}$, and $Ge_{5.6}Sb_{31.0}Se_{63.4}$) with particle sizes between 15nm and 30nm were fabricated using 3 different methods, all based on self-assembly of di-block co-polymers using "additive" and "subtractive" methods for the pattern transfer. Phase change materials were deposited by sputter deposition and by a newly developed spin-on process. In all cases arrays of isolated nanoparticles were formed. These fabrication techniques have the potential to produce even smaller

particles by changing the polymers. The particle size and spacing can be varied by using polymers with different block size and block ratio. The nanoparticle arrays crystallized at temperatures either slightly lower ($Ge_{15}Sb_{85}$ and $Ge_{5.6}Sb_{31.0}Se_{63.4}$) or slightly higher ($Ag_{7}In_{11}Sb_{48}Te_{34}$) than blanket films of the same material and deposited by the same method. This scaling behavior of phase change nanoparticles shows that the transition characteristics do not change dramatically if the materials are scaled down to dimensions in the 15-30 nm range, and that they behave similarly to blanket films. It was demonstrated that spin-on phase change materials can be designed that have properties favorable for solid state memory applications. These materials are particularly promising for processes that require via filling since high-aspect ratio filling capabilities have been demonstrated for these materials.[10] In summary, the phase change materials studied here posses scaling properties that will enable phase change solid state memory technology for several future technology nodes.

ACKNOWLEDGEMENTS

This research was carried out in part at The National Synchrotron Light Source, Brookhaven National Laboratory, which is supported by the U.S. Department of Energy, under Contract No. DE-AC02-98CH10886.

REFERENCES

[1] M. H. R. Lankhorst, B. W. S. M. M. Ketelaars, and R. A. M. Wolters, Nature Mater. **4**, 347 (2005).
[2] Y.-C. Chen, C. T. Rettner, S. Raoux, G. W. Burr, S. H. Chen, R. M. Shelby, M. Salinga, W. P. Risk, T. D. Happ, G. M. McClelland, M. Breitwisch, A. Schrott, J. B. Philipp, M. H. Lee, R. Cheek, T. Nirschl, M. Lamorey, C. F. Chen, E. Johseph, S. Zaidi, B. Yee, H. L. Lung, R. Bergmann, and C. Lam, Int. Electron Devices Meeting, San Francisco, USA, 2006.
[3] Y. H. Ya, J. H. Yi, H. Horii, J. H. Park, S. H. Joo, S. O. Park, U-In Chung, and J. T. Moon, 2003 Symp. on VLSI Technology and Circuits, Digest of Technical Papers, Kyoto, Japan, 2003.
[4] F. Pellizzer, A. Pirovano, F. Ottogalli, M. Magistretti, M. Scaravaggi, P. Zuliani, M. Tosi, A. Benvenuti, P. Besana, S. Cadeo, T. Marangon, R. Morandi, R. Piva, A. Spandre, R. Zonca, A. Modelli, E. Varesi, T. Lowrey, A. Lacaita, G. Casagrande, P. Cappeletti, and R. Bez, 2004 Symp. on VLSI Technology and Circuits, Digest of Technical Papers, Honolulu, USA, 2004.
[5] T. D. Happ, M. Breitwisch, A. Schrott, J. B. Philipp, M. H. Lee, R. Cheek, T. Nirschl, M. Lamorey, C. H. Ho, S. H. Chen, C. F. Chen, E. Johseph, S. Zaidi, G. W. Burr, B. Yee, Y. C. Chen, S. Raoux, H. L. Lung, R. Bergmann, and C. Lam, 2006 Symp. on VLSI Technology and Circuits, Digest of Technical Papers, Honolulu, USA, 2006.
[6] S. Raoux, C. T. Rettner, J. L. Jordan-Sweet, P. M. Mooney, G. M. McClelland, V. R. Deline, F. Houle, and A. Kellock, Workshop on Physics and Chemistry of Condensed Matter, San Francisco, CA, April 2005
[7] S. Raoux, C. T. Rettner, J. Jordan-Sweet, V. R. Deline, J. B. Philipp, and H. L. Lung, Proc. Europ. Conf. on Phase Change and Ovonic Science, Grenoble, France, 2006.
8 Y. Zhang, H.-S. P. Wong, S. Raoux, J. N. Cha, C. T. Rettner, L. E. Krupp, T. Topuria, D. J. Milliron, P. M. Rice, and J. L. Jordan-Sweet, Appl. Phys. Lett. **91**, 013104 (2007).
[9] J. N. Cha, Y. Zhang, H.-S. Wong, S. Raoux, C. Rettner, L. Krupp, and V. Deline, Chem. Mater. **2007**, 19, 839.
[10] D. J. Milliron, S. Raoux, R. M. Shelby, and J. Jordan-Sweet, Nature Mater. **6**, 352 (2007).